

DFT Study of the Interaction between the Ni²⁺ and Zn²⁺ Metal Cations and the 1,2-Dithiolene Ligands: Electronic, Geometric and Energetic Analysis

Glauber S. Melengate,^a Daniel G. S. Quattrociochi,^a José M. Siqueira Júnior,^{ib} ^a
 Stanislav R. Stoyanov,^{b,c} Leonardo M. Costa^{*,a,d} and Glaucio B. Ferreira^{ib} ^{*,a}

^aPrograma de Pós-Graduação em Química,
 Instituto de Química, Universidade Federal Fluminense,
 Outeiro de São João Batista, s/n 24020-141 Niterói-RJ, Brazil

^bNatural Resources Canada, Canmet ENERGY in Devon, 1 Oil Patch Drive,
 T9G 1A8 Devon, Alberta, Canada

^cDepartment of Chemical and Materials Engineering, University of Alberta,
 T6G 2V4 Edmonton, Alberta, Canada

^dDepartamento de Química Geral e Inorgânica, Instituto de Química,
 Universidade Estadual do Rio de Janeiro, Rua São Francisco Xavier, 524,
 Pavilhão Haroldo Lisboa da Cunha, 205509-000 Rio de Janeiro-RJ, Brazil

Density functional theory (DFT) (B3LYP/6-311++G(d,p)) calculations of the interacting strength 1,2-dithiolene anionic ligands with the [M(OH₂)₄]²⁺ and [M(OH₂)₂]²⁺ complexes (M = Ni and Zn) were performed. Three series of ligands were studied: compounds with an aromatic ring, with an ethylene moiety and with a heterocyclic ring. The ligands have substituents electron donors and acceptors by induction and resonance. Two substitution reactions were studied: the first is the substitution of two water molecules from the [M(OH₂)₆]²⁺ by a dithiolene anionic ligand (L²⁻) and the second is the substitution of two water molecules from the [M(OH₂)₄L] by another dithiolene anionic ligand. Geometric, electronic and energetic properties of the substituted aquacations are correlated with the metal-ligand affinity. All the substitution processes for both metal cations are spontaneous and are modulated by the electronic effect of each substituent of the ligand. Geometric parameters and chelation angle are correlated with the interaction strength. The energy decomposition analysis (EDA) results show that the electrostatic component is the main stabilizing term for the monosubstituted complexes, while for the disubstituted complexes the covalent term is the main stabilizing component. The polarization term is the main one to describe the covalent character. Natural bond orbital (NBO) shows the acid-base interaction nature of the metal-ligand bond.

Keywords: divalent metal cations, 1,2-dithiolene ligands, DFT, interaction analysis, EDA, NBO

Introduction

Metal dithiolene complexes have been extensively investigated since 1960 mainly due to their conducting, optical and magnetic properties.^{1,2} They are used in molecular devices, superconductors, dye-sensitized solar cells, catalyst for molecular hydrogen production, electronic recording disks and model compounds of more elaborated architectures, as in the active sites of

pyranopterin molybdenum enzymes.³⁻⁵ The dithiolene ligands are studied as elementary building blocks of enzymes, such as ureases (associated with the Ni²⁺ cation)⁶ and phospholipases (associated with the Zn²⁺ cation).⁷ They can also act as metalloligands toward other metallic centers.⁸ The metal-ligand interaction in the active site of these enzymes is responsible for some unique parameters as conformation, acid-base and the non-innocent redox behavior of the ligand. The variation of the substituents of the dithiolene ligand can completely change the electronic distribution and geometric arrangement of the model

*e-mail: glauciofb@vm.uff.br; lmcosta@id.uff.br

compound, directly influencing its action and performance in electrocatalyst processes.⁹

Experimental and computational studies have analyzed the interaction among divalent metal cations with large number of ligands.^{10,11} Soras *et al.*^{12,13} synthesized a nickel complex with an extended multi-sulfur dithiolene ligand. The structures obtained from X-ray diffraction indicate that Ni²⁺ ion is tetracoordinated with a square planar geometry. B3LYP calculations show that the methoxy groups are placed above and below the metal dithiolene core, due to stereochemical hindrance and are not formally bonded to the metal center. Drzewiecka-Antonik *et al.*¹⁴ analyzed the complexation of the Co²⁺, Ni²⁺ and Cu²⁺ metal cations with 2,4-dichlorophenoxyacetic acids. It was concluded by a combined density functional theory (DFT) and X-ray absorption near edge structure (XANES) analysis that, after the first and second ligand complexation, both octahedral and square planar interaction geometry can be obtained. Xia *et al.*¹⁵ studied the nature of the interaction between the Pt²⁺ and Pd²⁺ metal cations with dithiolene ligands by natural bond orbital (NBO) analysis. It was seen that the chemical bond, described as an acid-base interaction, has prominent donor-acceptor interactions between the ligand and the metal. Plazinski and Drach¹⁶ analyzed the bonding affinity between transition divalent metal cations (Zn²⁺, Cd²⁺, Cu²⁺, Mn²⁺ and Co²⁺) with amino acids molecules. The affinity order of each metal for the amino acid compounds was quantified in terms of the complexation Gibbs free energy. Tavassoli and Fattahi¹⁷ studied the interaction between an amino acid (histidine ligand) and divalent metal cations (Zn²⁺, Ca²⁺ and Mg²⁺). They observed that the electrostatic term is predominant in all metal-ligand interactions, but the strongest interaction occurred with the softest metal cation. In the previous works,^{18,19} the interaction between metal cations and neutral ligands was also studied. The alkaline earth metal cations showed larger affinity by ligands with large negative charge on the interacting atoms (O > N > S ligands). The metal-ligand affinity can be described in terms of geometrical (distance and angles), electronic (charge on specific atoms) and energetic (Gibbs free energy change, energy decomposition analysis, highest occupied molecular orbital (HOMO) and lowest unoccupied molecular orbital (LUMO) energies) parameters. All these terms correlate with the intensity of metal-ligand binding. It was also observed that the neighborhood groups of the interacting atom also modulate the metal-ligand affinity. Electron donor groups enhance the metal-ligand affinity, while electron withdrawing groups weaken the interaction.

In the present work the interaction between the Ni²⁺ and Zn²⁺ metal cations with 11 dithiolene ligands was

analyzed, as shown in Figure 1. Three series of dithiolene molecules were studied, differing by the organic moiety bonded to the two sulfur atoms: the first with an aromatic ring (Figures 1a-c, 1g), the second with an ethylene group (Figures 1d-f, 1h) and the last one with a heterocyclic ring (Figures 1j-k). To simulate the hydrated metal cations octahedral geometries were considered for all the hexaaquacomplexes, based on their most common coordination number in aqueous reaction medium, which represents the most usual conditions in coordination compound syntheses.^{20,21}

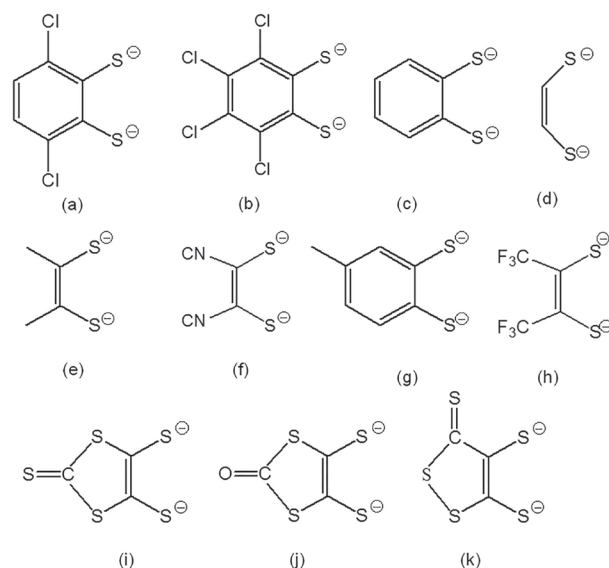


Figure 1. Chemical structures of the bidentate ligands with its respectively abbreviation: (a) 3,6-dichlorobenzene-1,2-dithiolate (Cl₂-bdt); (b) 3,4,5,6-tetrachlorobenzene-1,2-dithiolate (Cl₄-bdt); (c) benzene-1,2-dithiolate (bdt); (d) 1,2-ethylenedithiolate (edt); (e) 1,2-dimethyl-1,2-ethylenedithiolate (mdt); (f) maleonitrile-2,3-dithiolate (mnt); (g) toluene-3,4-dithiolate (tdt); (h) bis(trifluoromethyl)ethylenedithiolate (tfd); (i) 1,3-dithiole-2-thione-4,5-dithiolate (dmit); (j) 1,3-dithiole-2-one-4,5-dithiolate (dmio); (k) 1,2-dithiole-3-thione-4,5-dithiolate (dmt).

The ligands affinity order for each metal cation was determined by equations 1 and 2. In these equations, the substitution energy was determined for the change of two water molecules by a bidentate ligand in the coordination sphere of the metal aquacation [M(OH₂)₆]²⁺. This procedure was used for the first substitution reaction (equation 1) and for the second substitution reaction (equation 2), shown in Figure 2. A large number of studies report this methodology for the measurement of metal-ligand affinity.^{16,22-27}



The substitution energy was rationalized in terms of geometrical, electronic and energetic parameters inherent

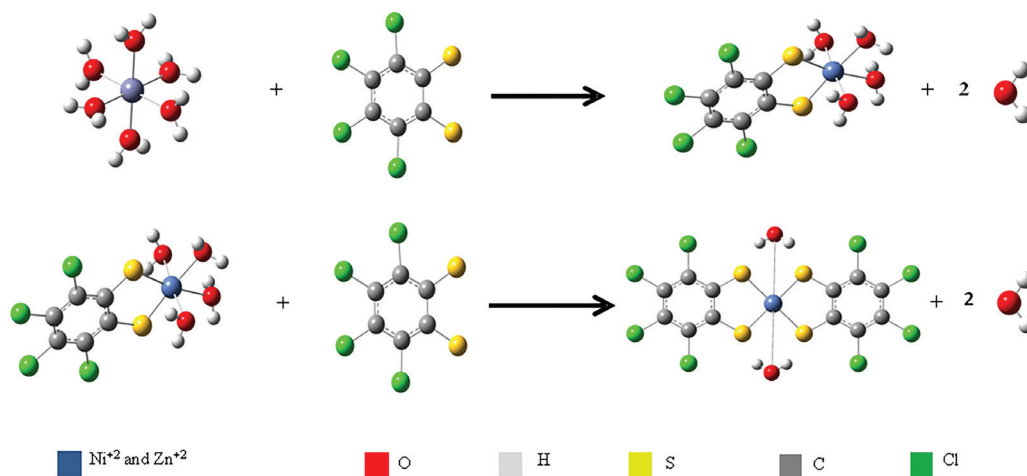


Figure 2. Complexation reactions between the $[M(OH_2)_6]^{2+}$ and the $[M(OH_2)_4L]$ species and the bdt dithiolene ligand (L^{2-}).

to the complexes and isolated ligands. The nature of the metal-ligand interaction was analyzed by the energy decomposition analysis (EDA) and NBO procedures. The influence of the substituent electronic effects was also evaluated (induction and resonance) of the ligands in the binding strength.

Methodology

DFT calculations were performed with the B3LYP functional²⁸ and the 6-311++G(d,p) basis set²⁹ using the Gaussian 09 software.³⁰ This DFT method generates optimization and energetic results in agreement with higher levels of theory.³⁰ By the rotation of single bonds, the structures of several conformers were calculated.³¹ Only the most stable conformers, among the several possible structures for each ligand, are reported. After full geometry optimization, vibrational mode calculations were performed to confirm that the optimized geometries are genuinely minimum points on the potential energy surface. For the Ni^{2+} complexes, the triplet state has been assumed, whereas for the Zn^{2+} the singlet state was used. The base set superposition error (BSSE) was performed by the counterpoise procedure.³² The B3LYP/6-311++G(d,p) method was also employed for the energy decomposition analysis using the GAMESS software.^{33,34} The EDA procedure decomposes the total interaction energy in five components: electrostatic (E_{Electro}), polarization (E_{Pol}), exchange (E_{xc}), dispersion (E_{Disp}) and Pauli repulsion (E_{Pauli}).³⁵ The sum of the polarization and exchange terms leads to the covalent interaction component. The NBO calculations were performed with the B3LYP/6-311++G(d,p) method to analyze the acid-base interaction in the substituted aqua complexes through the donor/acceptor energy.

Results and Discussion

Geometry optimization

The geometries of the 44 aqua complexes of Ni^{2+} and Zn^{2+} were fully optimized with the B3LYP/6-311++G(d,p) method. The optimized structures for the monosubstituted and disubstituted complexes are shown in Figures 3 and 4, respectively, and the final geometry symmetry in Table 1.

The analysis of Figure 3 shows that after the first ligand substitution the geometry of Ni^{2+} and Zn^{2+} aqua complexes continue to be octahedral, without any change on the aquacations coordinating axis. However, in the second ligand substitution the geometry of both Ni^{2+} and Zn^{2+} complexes is modified from the original octahedral $[M(OH_2)_6]^{2+}$. The Ni^{2+} disubstituted complexes present a quadratic geometry, which must be derived from the progressive elongation of the axial interactions with the water molecules that cause systematic d orbital energy stabilization. The Zn^{2+} disubstituted aqua complexes present tetrahedral coordination geometry. This geometry is favored when small metal cations interact with large ligands, as the dithiolene anions. In this case, the ligand-ligand repulsion promotes the geometry change because the octahedral stabilization is not enough to maintain the structure with six ligands. The Ni^{2+} and Zn^{2+} optimized geometries are in agreement with other theoretical studies.^{20,21,36,37} In a previous work with this class of ligands coordinated with Mg^{2+} and Ca^{2+} ions, the reorganization of the coordination sphere was also observed for some disubstituted complexes with reduced coordination number, such as penta and tetra coordination.¹⁹ These effects can be justified by the steric strain, where the second coordination of the bidentate ligand promotes a steric repulsion that leads to the elimination of water molecules from the coordination sphere.³⁸

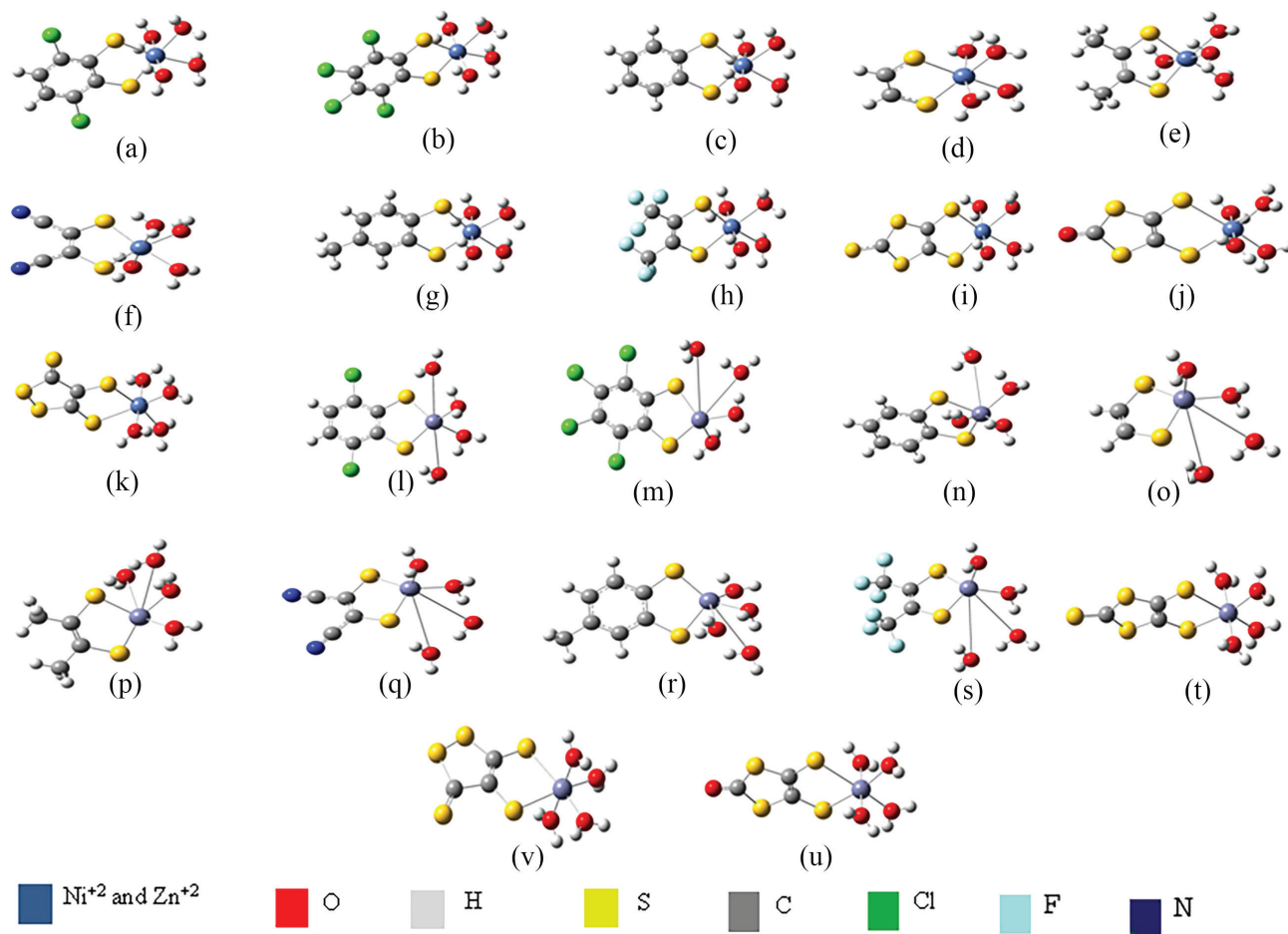


Figure 3. Optimized structures of the monosubstituted aquacomplexes: [Ni(OH₂)₄L] and [Zn(OH₂)₄L] with the Cl₂-bdt (a and l), Cl₄-bdt (b and m), bdt (c and n), edt (d and o), mdt (e and p), mnt (f and q), pdt (g and r), tfd (h and s), dmit (i and t), dmio (j and u) and dmt (k and v), respectively.

Ligand's affinity order

The affinity of each dithiolene ligand for the Ni²⁺ and Zn²⁺ cations was quantified by the interaction enthalpy (ΔH) and Gibbs free energy (ΔG) for the exchange of two water molecules for the bidentate ligand as shown in equations 1 and 2. The ΔH and ΔG results are shown in Table 1. The analysis of Table 1 presents that all the enthalpy and Gibbs free energy values are negative for the monosubstituted and disubstituted complexes showing that both substitution reactions are exothermic and spontaneous. For the first substitution reaction the interaction of each ligand is 9.09 ± 0.26 (ΔH) and 8.56 ± 0.18 (ΔG) kcal mol⁻¹ stronger with the Zn²⁺ cation than with the Ni²⁺ cation. For the ethylene ligands, the interacting order is edt > mdt > tfd > mnt, while for the aromatic ligands is bdt > tdt > Cl₂-bdt > Cl₄-bdt. The metal-ligand interacting enthalpy difference for edt and mdt ligands is 0.14 kcal mol⁻¹ and for the bdt and tdt is 0.01 kcal mol⁻¹. The enthalpy values are very close because the ligands differ only by methyl groups, which do not have significant electron donating or

accepting character. The interaction of each cation with the tfd and mnt, and with Cl₂-bdt and Cl₄-bdt ligands is weaker than with the previous ligands, respectively. This is explained by the electronic effect of the neighborhood of the anchor point of the ligands. The tfd, mnt, Cl₂-bdt and Cl₄-bdt have electron accepting groups that weaken the metal-ligand interacting strength by pulling electron density away from the anchoring atom, which destabilizes the bond. In the heterocyclic ligands the dmio ligand has a carbonyl group (C=O), whereas dmit and dmt have a thiocarbonyl group (C=S). The analysis of HOMO and LUMO frontier orbitals, of dmt and dmio molecules, show a prominent π character. This efficiently favors the electronic delocalization due to the large dimension of the S atoms (Figure 5). This effect reduces the electron density on the sulfur atoms weakening the metal-ligand interaction. This is not observed for the dmio ligand, where the p orbitals of the oxygen atom do not have the size and energy close to that of the sulfur atom. This difference disfavors the effective orbital overlap reducing the electronic dislocation effect.

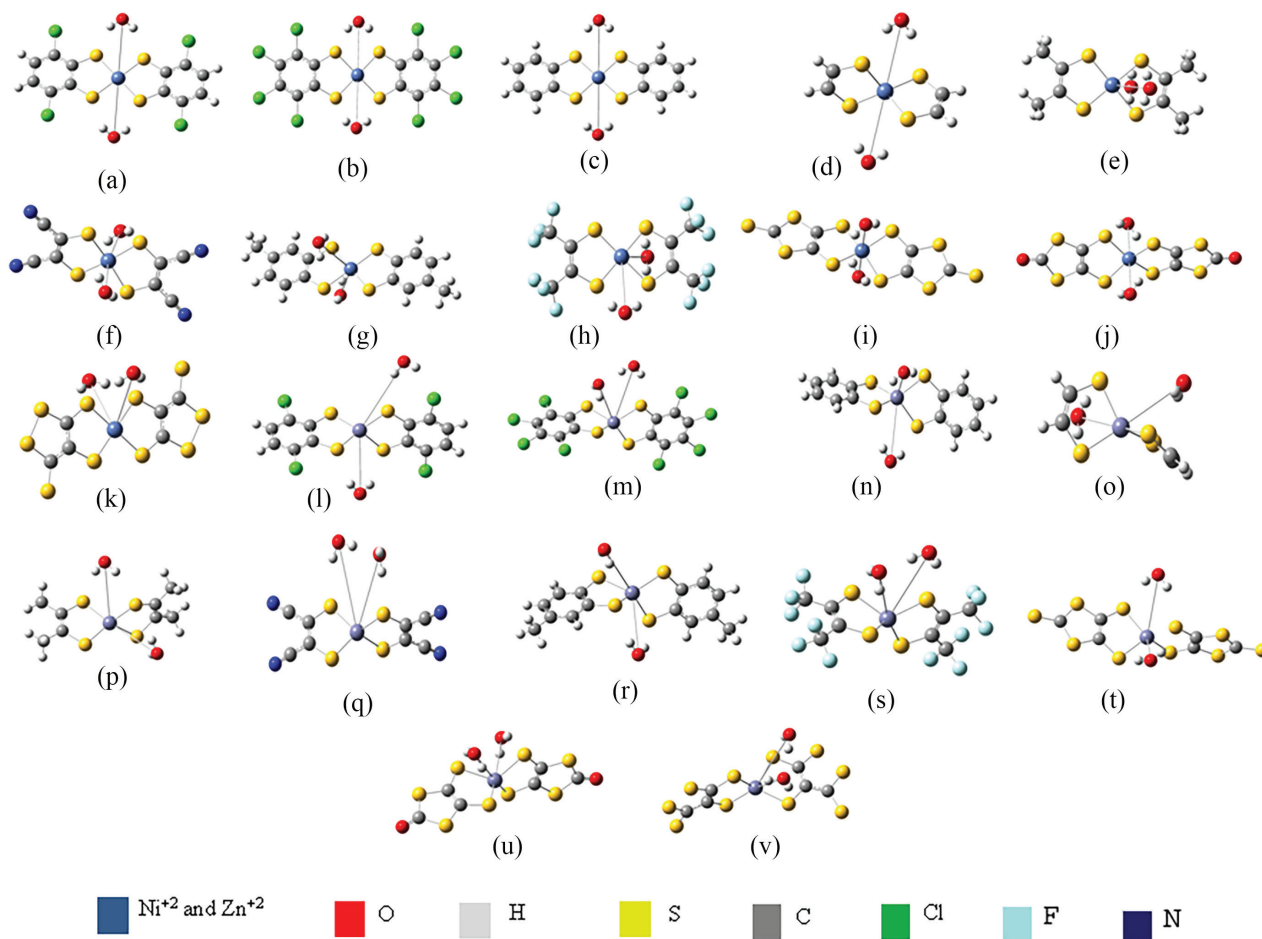


Figure 4. Optimized structures of the disubstituted aquacomplexes: $[\text{Ni}(\text{OH}_2)_2\text{L}_2]^{2-}$ and $[\text{Zn}(\text{OH}_2)_2\text{L}_2]^{2-}$ with the Cl_2 -bdt (a and l), Cl_4 -bdt (b and m), bdt (c and n), edt (d and o), mdt (e and p), mnt (f and q), pdt (g and r), tfd (h and s), dmit (i and t), dmio (j and u) and dmt (k and v), respectively.

In the second substitution reaction, the interacting aquacomplexes are neutral and interact with a divalent anion. Therefore, the second substitution reaction must have a smaller electrostatic stabilization term than the first substitution reaction, which leads to less negative values. The analysis of the second substitution reaction shows a distinct trend than the one for the first reaction. The Cl_2 -bdt, Cl_4 -bdt, bdt, edt, mdt, tfd ligands bind strongly to the Ni^{2+} cations, whereas the mnt, tdt, dmit, dmio, dmt have more favorable interaction with the Zn^{2+} cation. This is related with the ligands size around the coordination sphere of the metal cation. The analysis of Table 1 shows that for the second substitution reaction, ligands with electron acceptor groups have stronger interaction with the metal cations. For the ethylene ligands the interacting order is $\text{tfd} > \text{mnt} > \text{mdt} > \text{edt}$ for both the Ni^{2+} and Zn^{2+} cations. As the interaction is between neutral specie and a divalent anion, the electrostatic term does not play a relevant role as in the first substitution, being the covalent character more important. The presence of electron accepting groups decentralizes the charge on

the anchoring point of the ligand enhancing its softness, which favors the covalent interaction. This is also seen for the aromatic ligands, whereas the interaction order is Cl_4 -bdt $>$ Cl_2 -bdt $>$ bdt $>$ tdt, following the observation that ligands with electron acceptor groups strengthens the metal-ligand interaction.

The analysis of the ΔG values of Table 1 shows values negative in the substitution of 2 or 4 water molecules from the aquacations, confirming that these processes are spontaneous. In the monosubstituted complexes the interaction is stronger with the ethylene ligands, followed by the aromatic and heterocyclic molecules. In each set of ligands, the presence of electron accepting groups (Cl^- , F^- , CN^-) weaken the interaction strength with the metal center. As this interaction is between a cation and an anion, the electrostatic term plays an important role in the stabilization of the substituted molecules, as previously seen in the ΔH analysis. In the disubstituted complexes the interaction order changes. Ligands with electron accepting groups (tfd, mnt, Cl_4 -bdt, Cl_2 -bdt) have stronger interaction with the metal cations than ligands (mdt, tdt, edt, dmt, dmio,

Table 1. Optimized geometry symmetry of the mono and disubstituted aquacations (Geo), interaction enthalpy (ΔH), Gibbs free energy (ΔG), with the BSSE correction and entropic component ($-T\Delta S$) at 298 K, for the water exchange by one (monosubstituted complexes) or two ligands (disubstituted complexes) molecules

Ligand	Ni ²⁺			Zn ²⁺				
	Geo	$\Delta H /$ (kcal mol ⁻¹)	$\Delta G /$ (kcal mol ⁻¹)	$-T\Delta S /$ (kcal mol ⁻¹)	Geo	$\Delta H /$ (kcal mol ⁻¹)	$\Delta G /$ (kcal mol ⁻¹)	$-T\Delta S /$ (kcal mol ⁻¹)
Monosubstituted complex								
Cl ₂ -bdt	Oh	-361.91	-369.52	-7.61	Oh	-373.42	-379.74	-6.32
Cl ₄ -bdt	Oh	-349.27	-356.56	-7.29	Oh	-358.24	-365.64	-7.40
bdt	Oh	-376.59	-384.67	-8.08	Oh	-389.46	-395.69	-6.23
edt	Oh	-390.30	-397.55	-7.25	Oh	-399.77	-408.37	-8.60
mdt	Oh	-390.16	-398.70	-8.54	Oh	-395.17	-404.45	-9.28
mnt	Oh	-338.64	-346.52	-7.88	Oh	-347.95	-355.85	-7.90
tdt	Oh	-376.58	-384.78	-8.20	Oh	-382.22	-390.82	-8.60
tfd	Oh	-354.91	-362.64	-7.73	Oh	-362.47	-370.84	-8.37
dmit	Oh	-338.24	-346.30	-8.06	Oh	-346.23	-353.06	-6.83
dmio	Oh	-348.92	-357.10	-8.18	Oh	-363.40	-364.80	-4.40
dmt	Oh	-342.01	-350.40	-8.39	Oh	-349.24	-356.65	-7.41
Disubstituted complex								
(Cl ₂ -bdt) ₂	Qd	-91.80	-100.96	-9.16	Td	-87.50	-95.97	-8.47
(Cl ₄ -bdt) ₂	Qd	-92.70	-101.67	-8.97	Td	-89.10	-96.36	-7.56
(bdt) ₂	Qd	-90.55	-98.72	-8.17	Td	-88.16	-97.80	-9.64
(edt) ₂	Qd	-83.82	-91.78	-7.96	Td	-82.84	-92.16	-9.32
(mdt) ₂	Qd	-87.54	-97.67	-13.13	Td	-85.64	-94.75	-9.11
(mnt) ₂	Qd	-89.09	-99.65	-10.56	Td	-89.66	-100.75	-11.09
(tdt) ₂	Qd	-83.87	-91.02	-8.15	Td	-84.40	-94.01	-9.61
(tfd) ₂	Qd	-94.91	-104.41	-9.50	Td	-93.77	-104.10	-10.33
(dmit) ₂	Qd	-76.00	-86.30	-10.30	Td	-81.69	-92.38	-10.69
(dmio) ₂	Qd	-78.19	-88.26	-10.07	Td	-78.72	-89.26	-10.54
(dmt) ₂	Qd	-81.24	-91.19	-9.97	Td	-85.55	-94.96	-9.41

Geo: geometry; Oh: octahedral; Qd: quadratic; Td: tetrahedral; Cl₂-bdt: 3,6-dichlorobenzene-1,2-dithiolate; Cl₄-bdt: 3,4,5,6-tetrachlorobenzene-1,2-dithiolate; bdt: benzene-1,2-dithiolate; edt: 1,2-ethylenedithiolate; mdt: 1,2-dimethyl-1,2-ethylenedithiolate; mnt: maleonitrile-2,3-dithiolate; tdt: toluene-3,4-dithiolate; tfd: bis(trifluoromethyl)ethylenedithiolate; dmit: 1,3-dithiole-2-thione-4,5-dithiolate; dmio: 1,3-dithiole-2-one-4,5-dithiolate; dmt: 1,2-dithiole-3-thione-4,5-dithiolate.

dmit). In the second substitution reaction the interaction is between a neutral metal center, softer species than the metal cation in the first substitution reaction, and a dianion. In this case, the interaction has a larger covalent character and softer ligands will have a stronger interaction. As the electron accepting groups decentralize the negative charge on the tfd, mnt, Cl₄-bdt, Cl₂-bdt ligands, they must have the largest interacting strength.

Some trends on the ΔG^{298} values were also found in a previous work with the dithiolate ligands complexed with the Mg²⁺ and Ca²⁺ ions.¹⁹ Figure 6 shows the graphics of the first and second substitution Gibbs free energy of ethylenic and aromatic dithiolene. In the first substitution, it was observed that there was a greater stability of the

complexes containing ligands without electron acceptor groups. In addition, the transition metal complexes were more stabilized than the studied alkaline earth metal ions. In the case of the second substitution, where a change in the coordinate sphere for the Mg²⁺ and Ca²⁺ ions was observed, it was noticed a trend change on the stability for the same ligands, while Ni²⁺ and Zn²⁺ ions showed the same tendency for the different analyzed ligands. This is justified by the maintenance of the number of ligands coordinated to the ions even if there is a change of coordination type, quadratic for nickel and tetrahedral for zinc. However, it was also confirmed a greater stabilization of the complexes formed in the second substitution for the Ni²⁺ and Zn²⁺ ions than for the Mg²⁺ and Ca²⁺ ions.

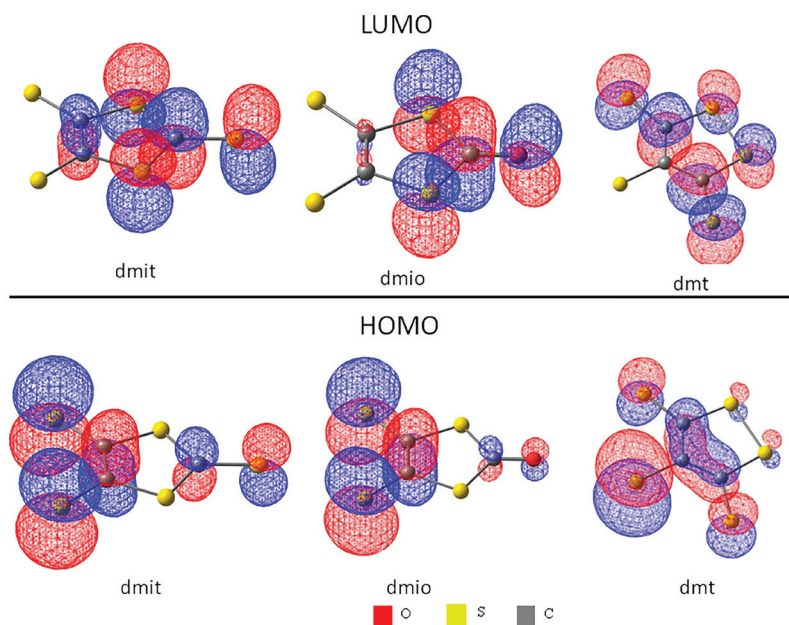


Figure 5. HOMO/LUMO molecular orbitals of dmit, dmio and dmt ligands.

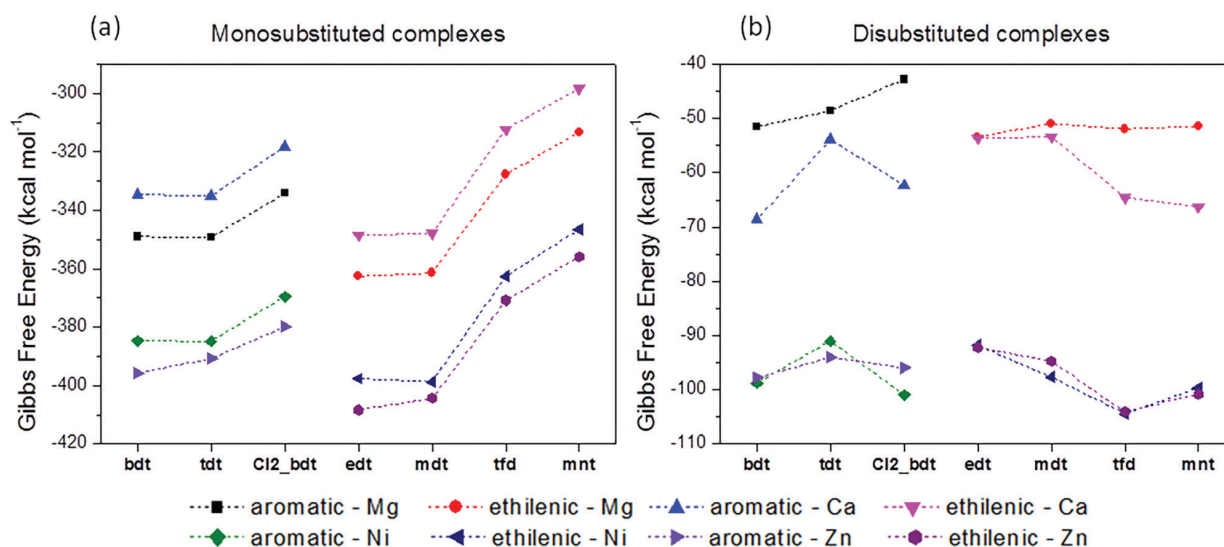


Figure 6. Gibbs free energy, in kcal mol⁻¹, for the monosubstituted (a) and disubstituted (b) ethylenic and aromatic dithiolene complexes.

Table 1 also exhibits the entropic parameter ($-T\Delta S$) values for each substitution reaction. The analysis of Table 1 shows that all the entropic contributions are negative for the first and second ligands substitution. In the substitution reaction (equations 1 and 2) it is possible to observe that the number of products is larger than the reactants, due to the metal cation coordination with a divalent ligand, which release two water molecules. This confirms the increase of the system disorder for the chelating ligands. It is possible to check that all the $-T\Delta S$ values for the second substitution is 1.99 ± 1.51 kcal mol⁻¹ more negative than for the first substitution. This may be related to the optimized geometries of each complex. In the

second substitution reaction the reactants have octahedral coordination geometry, while the products are quadratic or tetrahedral with a smaller coordination number. The bond elongation with the water molecules favors the system disorder and justifies the most negative $-T\Delta S$ values. It is also possible to associate with the electronic distribution on the interacting species. In the first reaction a divalent cation interacts with a divalent anion, with a strong electrostatic character, which may organize the system. In the second substitution reaction, softer species interact among themselves (neutral metal center and a dianion). In this case, a more dispersed electronic cloud forms the bond, and this may be favored by the entropic stabilization.

Chelate effect

The chelate effect shows that the interaction of a metal center with a polydentate ligand has a larger stabilization term than with the equivalent number of monodentate ligands. It can be correlated with the entropy variation between the chelate and the monodentate ligands in diluted solutions. Generally, chelation results in an increase of system free molecules that is entropically favored. This is not observed with the monodentate ligands, where the number of species in reactants and products is the same.³⁷ Additionally, the chelate effect also influences the kinetics of the metal-ligand interaction. When a monodentate ligand is bounded to a metal center and this bond breaks, the ligand returns to the media and there is a small probability of the interaction return. When a chelate ligand is bonded to a metal center and one bond breaks, the other anchoring points continue to make the metal-ligand interaction and the broken bond may return,³⁹ favoring the chelate complex stabilization. The chelate effect was measured by equation 3, where a dithiolene ligand acts as two monodentate ligands for two metal aquacenters, as shown in Figure 7. The ΔH and ΔG^{298} results are listed in Table 2.



Table 2. Enthalpy (ΔH), Gibbs free energy (ΔG^{298}) and entropic component ($-\text{T}\Delta S$) at 298 K for the interaction between the monodentate edt ligand (L^{2-}) and the $[\text{Ni}(\text{OH}_2)_6]^{2+}$ and $[\text{Zn}(\text{OH}_2)_6]^{2+}$ cations

	$\Delta H /$ (kcal mol ⁻¹)	$\Delta G^{298} /$ (kcal mol ⁻¹)	$-\text{T}\Delta S /$ (kcal mol ⁻¹)
$[\text{Ni}(\text{OH}_2)_6]^{2+}$	-356.37	-358.55	-2.18
$[\text{Zn}(\text{OH}_2)_6]^{2+}$	-376.23	-379.38	-3.15

The chelating energy can be obtained through the energy difference between the ligand acting as a bidentate (Table 1) and as a monodentate (Table 2) specie. For the interaction of the edt ligand with the Ni²⁺ aquacation the chelation energy is stabilized with 33.93 (ΔH) and 39.00 (ΔG) kcal mol⁻¹. For the interaction with the Zn²⁺ aquacation the chelation energy

is stabilized with 23.54 (ΔH) and 28.99 (ΔG) kcal mol⁻¹. It is also possible to observe that the term $-\text{T}\Delta S$ is less negative for the monodentate than for the bidentate edt ligand. The $-\text{T}\Delta S$ term changes from -7.25 (bidentate) to -2.18 kcal mol⁻¹ (monodentate) and -8.60 (bidentate) to -3.15 kcal mol⁻¹ (monodentate), for the Ni²⁺ and Zn²⁺ complexes, respectively, for the first substitution reaction. This is mostly driven by the number of species in the reactants and products of each reaction and shows that the bidentate coordination is more thermodynamically favorable than the monodentate mode.

Energy decomposition analysis (EDA)

The EDA method decomposes the metal-ligand total interaction energy (E_{Tot}) into five components: the electrostatic, E_{Elec} , (opposite charge attraction), polarization, E_{Pol} , (orbital overlap), exchange, E_{Xc} , (parallel spin stabilization), dispersion, E_{Disp} , (long range interactions) and Pauli repulsion, E_{Pauli} , (electronic repulsion) terms. The bond among each aquacation $[\text{M}(\text{OH}_2)_4]^{2+}$ and $[\text{M}(\text{OH}_2)_2\text{L}]$ (first fragment) and the ligand (second fragment) was decomposed and analyzed. In Table 3, the EDA results are shown for both the Ni²⁺ and Zn²⁺ cations and for the first and second substitution reactions. The total energy (E_{Tot}) interaction order is the same obtained for the ΔH analysis. The E_{Tot} term involves the energy calculation of the fragments together and in a large distance (without interaction), with the same optimized geometry.

In the first substitution reaction the electrostatic term is the major one corresponding to 65.90 ± 1.38% (Ni²⁺) and 64.51 ± 0.97% (Zn²⁺) of the stabilizing components (E_{Elec} , E_{Pol} and E_{Xc}), in agreement with other studies.⁴⁰ This is due to the interaction between two charged species (divalent cation and anion). The electronic nature of the ligands substituents directly influences the E_{Elec} magnitude, as also previously seen for ΔH . Ligands with electron accepting groups (Cl_2 -bdt, Cl_4 -bdt, mnt and tfd), reduce the negative charge on the interacting S atoms, leading to a less stable interaction with the metal cations. The polarization component represents 20.12 ± 1.53 (Ni²⁺) and 23.43 ± 1.35% (Zn²⁺) of E_{Tot} , with

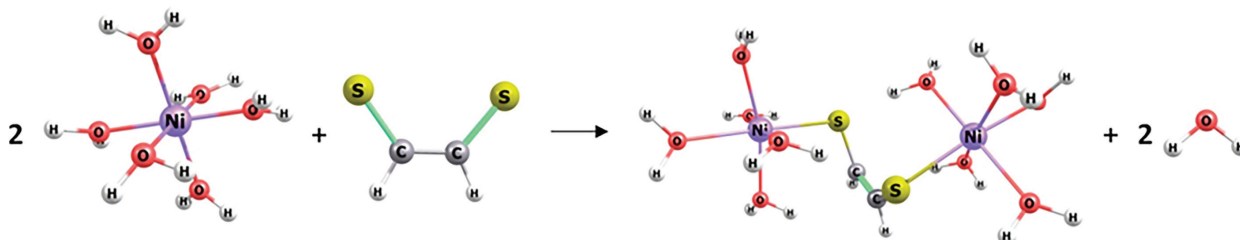


Figure 7. Complexation reaction between the Ni²⁺ aquacation and the edt ligand (L^{2-}).

a variation less than 19 kcal mol⁻¹, according to type of ligand. The exchange and dispersion terms represent about 10 and 3%, respectively, of the total interaction energy for both cations. The Pauli repulsion term is reduced for ligands with electron accepting substituents. This term destabilizes the cation-ligand interaction. Table 3 also lists the variation of the Pauli repulsion term with the distinct dithiolate ligands. It shows that the Pauli repulsion is larger for the aquacomplexes that have strong interaction with the ligands. This is probably resulting from the large electronic repulsion between the ligand and metal electronic density that increase due to the small metal-ligand distance. It is observed that both Cl₄-bdt and tfd ligands have reduced Pauli repulsion values compared to the other aromatic dithiolate ligands. This is

due to the inductive effect of the electron density withdrawal of the Cl and F atoms. In the second substitution reaction it is possible to see that the electrostatic term continues to be individually the largest one, but with a reduced magnitude for E_{Tot}, representing 44.30 ± 0.88 (Ni²⁺) and 45.20 ± 1.31% (Zn²⁺) of the metal-ligand interaction. The comparison among the electrostatic energies for the monosubstituted and disubstituted complexes indicates the reduction of 295.63 ± 34.42 (Ni²⁺) and 311.13 ± 23.95 kcal mol⁻¹ (Zn²⁺). In the second substitution, the interaction is between a neutral specie and an anion, which reduces the stabilization energy due to opposite charge attraction. In the second substitution the polarization and dispersion terms also reduce its magnitude and the exchange term is enhanced.

Table 3. Total interaction energy (E_{Tot}), electrostatic (E_{Elec}), polarization (E_{Pol}), exchange (E_{Xc}), dispersion (E_{Disp}) and Pauli repulsion (E_{Pauli}) components of the interaction, obtained with the EDA calculation

Ligand	Ni ²⁺ (Oh)						Zn ²⁺ (Oh)					
	E _{Tot} / (kcal mol ⁻¹)	E _{Elec} / (kcal mol ⁻¹)	E _{Pol} / (kcal mol ⁻¹)	E _{Xc} / (kcal mol ⁻¹)	E _{Disp} / (kcal mol ⁻¹)	E _{Pauli} / (kcal mol ⁻¹)	E _{Tot} / (kcal mol ⁻¹)	E _{Elec} / (kcal mol ⁻¹)	E _{Pol} / (kcal mol ⁻¹)	E _{Xc} / (kcal mol ⁻¹)	E _{Disp} / (kcal mol ⁻¹)	E _{Pauli} / (kcal mol ⁻¹)
Monosubstituted complexes [M(OH) ₂ L]												
Cl ₂ -bdt	-523.55	-493.19	-150.06	-80.43	-23.27	272.31	-523.55	-505.24	-178.43	-75.42	-22.65	258.18
Cl ₄ -bdt	-509.07	-475.06	-150.57	-78.00	-22.24	265.69	-509.07	-484.55	-179.38	-70.95	-20.52	246.34
bdt	-540.76	-513.12	-149.76	-83.40	-24.84	279.26	-540.76	-520.67	-179.63	-77.24	-24.02	260.80
edt	-557.30	-540.60	-138.60	-87.82	-26.36	288.09	-557.30	-538.97	-174.08	-76.86	-24.51	257.12
mdt	-551.91	-533.36	-151.27	-87.54	-26.36	289.42	-551.91	-528.31	-178.13	-74.31	-24.17	253.00
mnt	-446.69	-436.10	-165.37	-73.49	-22.22	252.16	-496.41	-469.03	-197.37	-64.88	-20.44	225.97
tdt	-492.90	-511.61	-152.03	-83.36	-24.83	278.93	-540.33	-512.76	-181.66	-72.57	-23.01	249.67
tfd	-483.07	-486.32	-163.28	-80.00	-24.16	270.69	-533.43	-501.82	-195.39	-71.01	-19.87	244.21
dmit	-446.85	-459.95	-138.96	-73.59	-23.50	249.14	-500.62	-461.17	-174.37	-61.99	-21.54	223.50
dmio	-458.87	-478.21	-136.66	-75.88	-23.39	255.27	-508.37	-487.35	-168.71	-71.35	-22.89	225.97
dmt	-450.43	-465.35	-145.02	-76.17	-23.44	259.55	-504.35	-466.04	-178.00	-62.67	-21.44	241.93
Disubstituted complexes [M(OH) ₂ L ₂] ²⁻												
(Cl ₂ -bdt) ₂	-176.70	-198.53	-139.05	-86.75	-21.48	269.11	-164.18	-183.90	-122.50	-76.95	-17.03	236.21
(Cl ₄ -bdt) ₂	-178.04	-198.74	-140.02	-85.61	-21.19	267.52	-162.45	-184.98	-126.32	-79.39	-16.72	244.96
(bdt) ₂	-176.04	-198.15	-137.76	-89.28	-22.30	271.46	-164.96	-189.90	-126.28	-86.77	-19.04	257.01
(edt) ₂	-178.06	-205.44	-134.00	-92.35	-23.12	274.85	-161.05	-188.82	-125.00	-89.62	-19.66	262.05
(mdt) ₂	-165.46	-176.33	-134.34	-79.50	-20.31	244.90	-156.66	-188.92	-124.71	-94.76	-20.49	272.21
(mnt) ₂	-185.79	-204.55	-143.63	-83.38	-20.30	266.08	-169.44	-188.47	-113.54	-72.97	-17.43	222.96
(tdt) ₂	-166.22	-178.59	-135.31	-78.78	-19.70	246.16	-157.69	-182.19	-131.76	-87.75	-17.95	261.95
(tfd) ₂	-184.89	-205.12	-137.32	-83.17	-20.98	261.70	-170.22	-193.95	-121.39	-78.50	-17.38	241.00
(dmit) ₂	-177.04	-190.49	-145.12	-84.16	-20.53	263.26	-164.02	-184.84	-127.04	-83.86	-18.16	249.89
(dmio) ₂	-179.49	-196.01	-143.69	-85.99	-21.21	267.42	-161.13	-185.34	-129.12	-86.82	-18.80	258.94
(dmt) ₂	-172.58	-189.02	-137.92	-80.65	-20.39	255.39	-162.10	-182.22	-126.08	-80.51	-17.65	244.36

Oh: octahedral; Qd: quadratic; Td: tetrahedral; Cl₂-bdt: 3,6-dichlorobenzene-1,2-dithiolate; Cl₄-bdt: 3,4,5,6-tetrachlorobenzene-1,2-dithiolate; bdt: benzene-1,2-dithiolate; edt: 1,2-ethylenedithiolate; mdt: 1,2-dimethyl-1,2-ethylenedithiolate; mnt: maleonitrile-2,3-dithiolate; tdt: toluene-3,4-dithiolate; tfd: bis(trifluoromethyl)ethylenedithiolate; dmit: 1,3-dithiole-2-thione-4,5-dithiolate; dmio: 1,3-dithiole-2-one-4,5-dithiolate; dmt: 1,2-dithiole-3-thione-4,5-dithiolate.

The ionic and covalent character of the metal-ligand interaction were also compared for the monosubstituted and disubstituted complexes (Figure 8). The ionic character was accounted as the electrostatic term, while the covalent character was measured as the sum of the polarization and exchange components of the total interaction energy.

In Figure 8 a graph of the ionic and covalent terms of the metal-ligand interaction is shown. The analysis of Figures 8a and 8b shows that for both the monosubstituted Ni²⁺ and Zn²⁺ aquacomplexes the interaction has a predominant ionic character. The nature of this interaction can be explained due to the two charged parts which are interacting: the metal aquacation [M(OH₂)₆]²⁺ and the dithiolene ligands (dianions), which stabilize the complex due to opposite charge attraction. The magnitude of the covalent component is almost half of the ionic term for all the ligands. The analysis of Figures 8c and 8d also shows that for the disubstituted Ni²⁺ and Zn²⁺ complexes, the covalent character is predominant. The values of the covalent term are similar for both the monosubstituted and disubstituted aquacomplexes, whereas the ionic component has a large reduction for the disubstituted complexes. The

disubstituted complexes present an interaction between neutral specie and a dianion that favors the major orbital overlap stabilization. This observation is opposite to that found for the disubstituted complexes of Mg²⁺ and Ca²⁺ cations.¹⁷ The disubstituted species present a smaller covalent component with closer values to the ionic term.

Geometrical, electronic and energetic parameters analysis

In the sections above the ligand affinity order for the Ni²⁺ and Zn²⁺ cations were analyzed. The interaction strength order can be associated with some geometrical, electronic and energetic parameters of the complexed aquacations to justify its intensity. As geometrical parameters the metal-ligand bond distance and the chelation angle for the monosubstituted and disubstituted aquacomplexes were analyzed. The metal-ligand interacting distances are shown in Table 4. In Cambridge Crystallography Data Centre (CCDC) a large number of S binding ligands coordinated with the Zn²⁺ (47 structures) and Ni²⁺ (ca. 1200 structures) cations were found. The Ni-S distances of complexes are 2.118-2.190 Å, whereas 2.316-2.344 Å for Zn-S compounds.

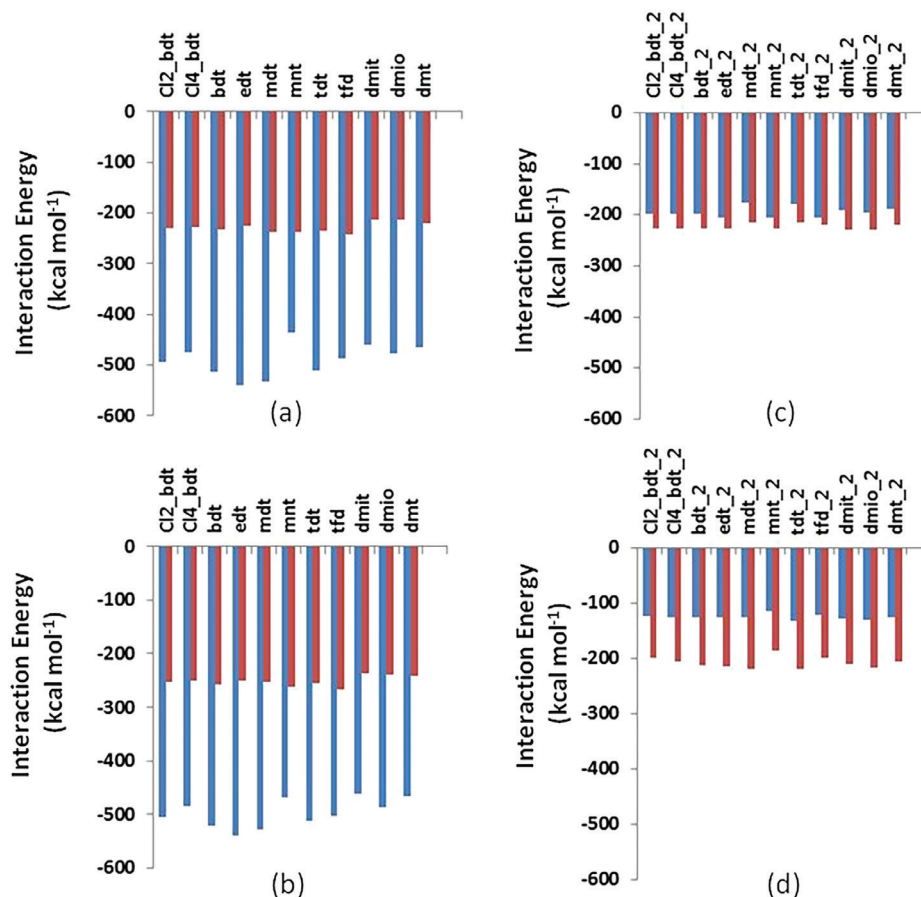


Figure 8. Ionic (blue) and covalent (red) components of the metal-ligand interaction, in kcal mol⁻¹, for the monosubstituted (a) [Ni(OH₂)₄L] and (b) [Zn(OH₂)₄L], disubstituted (c) [Ni(OH₂)₂L₂]²⁻ and (d) [Zn(OH₂)₂L₂]²⁻ aquacations.

Table 4. Metal-ligand bond distances (D_{M-L1} , D_{M-L2} , D_{M-L3} , D_{M-L4}), of the monosubstituted $[\text{Ni}(\text{OH}_2)_4\text{L}]$, $[\text{Zn}(\text{OH}_2)_4\text{L}]$ and disubstituted $[\text{Ni}(\text{OH}_2)_2\text{L}_2]^{2-}$ and $[\text{Zn}(\text{OH}_2)_2\text{L}_2]^{2-}$ complexes

	$D_{M-L1} / \text{Å}$		$D_{M-L2} / \text{Å}$			
	$D_{M-L2} / \text{Å}$		$D_{M-L3} / \text{Å}$		$D_{M-L4} / \text{Å}$	
	[M(OH ₂) ₄ (L)]		[M(OH ₂) ₂ (L) ₂] ²⁻			
	Ni ²⁺ (Oh)		Ni ²⁺ (Qd)			
Cl ₂ -bdt	2.306	2.315	2.232	2.232	2.232	2.232
Cl ₄ -bdt	2.304	2.313	2.226	2.226	2.226	2.226
bdt	2.317	2.329	2.247	2.247	2.247	2.247
edt	2.455	2.460	2.345	2.343	2.343	2.345
mdt	2.313	2.322	2.258	2.258	2.240	2.240
mnt	2.326	2.337	2.232	2.232	2.225	2.225
tdt	2.319	2.329	2.238	2.239	2.253	2.253
tfd	2.437	2.437	2.235	2.231	2.218	2.231
dmit	2.341	2.354	2.253	2.253	2.252	2.253
dmio	2.323	2.355	2.252	2.252	2.252	2.252
dmt	2.346	2.358	2.264	2.235	2.240	2.249
	Zn ²⁺ (Oh)		Zn ²⁺ (Td)			
Cl ₂ -bdt	2.268	2.274	2.378	2.377	2.373	2.350
Cl ₄ -bdt	2.254	2.266	2.385	2.385	2.349	2.352
bdt	2.244	2.311	2.385	2.385	2.406	2.362
edt	2.258	2.294	2.437	2.411	2.411	2.438
mdt	2.247	2.282	2.432	2.400	2.398	2.357
mnt	2.265	2.292	2.388	2.405	2.377	2.384
tdt	2.247	2.289	2.355	2.392	2.397	2.425
tfd	2.248	2.273	2.359	2.353	2.393	2.397
dmit	2.276	2.300	2.425	2.377	2.401	2.400
dmio	2.292	2.303	2.401	2.420	2.420	2.401
dmt	2.252	2.306	2.443	2.338	2.441	2.365

Å: Angström; Oh: octahedral; Qd: quadratic; Td: tetrahedral; Cl₂-bdt: 3,6-dichlorobenzene-1,2-dithiolate; Cl₄-bdt: 3,4,5,6-tetrachlorobenzene-1,2-dithiolate; bdt: benzene-1,2-dithiolate; edt: 1,2-ethylenedithiolate; mdt: 1,2-dimethyl-1,2-ethylenedithiolate; mnt: maleonitrile-2,3-dithiolate; tdt: toluene-3,4-dithiolate; tfd: bis(trifluoromethyl)ethylenedithiolate; dmit: 1,3-dithiole-2-thione-4,5-dithiolate; dmio: 1,3-dithiole-2-one-4,5-dithiolate; dmt: 1,2-dithiole-3-thione-4,5-dithiolate.

The analysis of Table 4 shows an asymmetry in the metal ligand bond distances for almost all the mono- (octahedral) and the disubstituted (Ni²⁺ quadratic, and Zn²⁺ tetrahedral) complexes. This indicates that the metal center interacts stronger with one S anchor point than with the other S binding atom of each dithiolene ligand. In the monosubstituted complexes this difference is 0.011 ± 0.01 and 0.031 ± 0.02 Å for the Ni²⁺ and Zn²⁺ compounds, respectively. In the disubstituted complexes this difference is 0.004 ± 0.01 and 0.022 ± 0.04 Å for the Ni²⁺ and Zn²⁺ derivatives, respectively. The Ni²⁺ disubstituted complexes with Cl₂-bdt, Cl₄-bdt, bdt, edt, dmit and dmio showed the same metal-ligand distances in the quadratic geometry. For both the mono- and disubstituted molecules, the Ni²⁺ complexes have smaller variation of bond length than the Zn²⁺ compounds. It is also possible to observe that in the

monosubstituted complexes all the Zn–S distances are 0.08 ± 0.05 Å smaller than the Ni–S bond lengths. For the disubstituted complexes it is noted that all the metal-ligand interacting distances are 0.100 ± 0.04 Å smaller than the monosubstituted ones. This is probably due to the reduction of the coordination number of the metal cation from 6 (octahedral) to 4 (quadratic or tetrahedral). With a reduced number of ligands around the metal center, the acid-base interaction is more effective and reduces the metal-ligand bond distance. The substituent group attached to the anchor atom is also important in the determination of the binding distance.

In Table 5 the chelation angles are listed for the mono- and disubstituted complexes. The analysis of the chelation angles shows larger values for the monosubstituted Zn²⁺ complexes than for the Ni²⁺ analog compounds. This can be

related with the interaction strength and metal-ligand bond length. As the Zn²⁺ cation has a stronger interaction with the dithiolene ligands and a smaller Metal–S bond length, the chelation angle should be larger to better accommodate the electron density around the metal center. In the disubstituted complexes all the chelation angles are smaller than in the monosubstituted molecules. This is probably due to the change of the final geometry. As in the disubstituted complexes the covalent character is enhanced, the orbital overlap must reduce the values of the chelation angles.

The geometric results presented so far are in agreement with the work of Hancock and Martell³⁸ where an enhanced coordination number results in an increase of the bond distance minimizing the steric strain in the substituted complexes. However, the change in geometry observed with the coordination of bulky ligands, from octahedral to quadratic or tetrahedral, can be correlated with the thermodynamic radius: the radius of the metallic ions when hydrated (*r*). For example, considering the hydrated species with [M(H₂O)₆]²⁺, we have the following correlation: *r*_{Ni2+} = 0.715, *r*_{Zn2+} = 0.74, *r*_{Mg2+} = 0.76 and *r*_{Ca2+} = 1.12.²¹ It was observed that structures with smaller thermodynamic cations present larger distortion of their geometry for disubstituted systems. This effect, as noted in the topic of optimized geometry, was strongly observed for the smallest cations. This observation can be understood by a more restricted volume in the second anchorage of the dithiolates sulfur atoms and a larger steric strain when the ring is formed. The rule of the ligands interaction with metal is limited to the size and the systems selectivity as a function of the steric strain. This may explain the displacement of

water molecules in some structures, specifically in the case of the second substitution of the ligand with geometry alteration.³⁸ In contrast, when there is a larger steric efficiency, that is, a higher affinity of the ion and a smaller distortion of its structure, it was not observed the change in the complex geometry. This can be better understood by analyzing the data for the complexes containing the bdt ligand. In the monosubstituted, the bdt has larger M–L distance and larger angle, which represents a less restricted volume. Therefore, the coordination of the second binding atom is more favorable than the others with higher stability of the substituted complex, which can be verified by more negative substitution energies. In a previous work¹⁹ with the dithiolate ligands containing the alkaline earth metals Mg²⁺ and Ca²⁺, it was observed that the cations with smaller thermodynamic radius showed a change in the coordination sphere. The only one that maintained the structure upon entering the second bidentate ligand was the Ca²⁺ cation. The thermodynamic radii of Mg²⁺ and Zn²⁺ are very close, and it was found that both underwent the same change in the coordination sphere from octahedral to tetrahedral from the first to the second substitution. In the first substitution, the chelation angle in the Zn complex was larger leading to a more stable structure by minimizing the effects of steric repulsion and allowing the ligands to have a larger approximation to the metal center. As a result of this approach, a more negative value of enthalpy and Gibbs free energy was obtained for the octahedral structure formation [Zn(H₂O)₄L]²⁺. In the second substitution, both Mg, Zn and Ni complexes with bdt showed a change of geometry from octahedral to tetracoordinated because they have a lower

Table 5. Chelation angle for the Ni²⁺ and Zn²⁺ complexes for the first ([M(OH)₂(L)]⁺) and second ([M(OH)₂(L)₂]²⁺) ligands substitution. In the disubstituted complexes, the sulfur atoms of each ligand are labeled as S₁, S_{1'} and S₂, S_{2'}.

Ligand	[M(OH) ₂ (L)] ⁺ / degree		[M(OH) ₂ (L) ₂] ²⁺ / degree			
	S–Ni–S	S–Zn–S	S ₁ –Ni(Qd)–S _{1'}	S ₂ –Ni(Qd)–S _{2'}	S ₁ –Zn(Td)–S _{1'}	S ₂ –Zn(Td)–S _{2'}
Cl ₂ -bdt	92.29	99.26	90.17	90.17	90.21	91.38
Cl ₄ -bdt	91.98	99.68	90.18	90.18	88.88	91.35
bdt	92.83	99.83	90.08	90.80	91.13	91.40
edt	86.36	101.35	90.52	90.52	90.88	90.88
mdt	91.90	99.00	89.23	89.66	88.19	91.43
mmt	92.74	99.94	91.45	91.52	91.10	92.24
tdt	92.93	100.18	90.41	90.24	92.07	88.96
tfd	85.02	99.21	89.76	90.07	91.20	88.54
dmit	94.18	101.60	93.10	93.10	93.51	93.40
dmio	94.11	100.72	93.07	93.07	92.07	92.06
dmt	93.12	100.58	90.86	91.03	91.70	90.97

Qd: quadratic; Td: tetrahedral; Cl₂-bdt: 3,6-dichlorobenzene-1,2-dithiolate; Cl₄-bdt: 3,4,5,6-tetrachlorobenzene-1,2-dithiolate; bdt: benzene-1,2-dithiolate; edt: 1,2-ethylenedithiolate; mdt: 1,2-dimethyl-1,2-ethylenedithiolate; mmt: maleonitrile-2,3-dithiolate; tdt: toluene-3,4-dithiolate; tfd: bis(trifluoromethyl) ethylenedithiolate; dmit: 1,3-dithiole-2-thione-4,5-dithiolate; dmio: 1,3-dithiole-2-one-4,5-dithiolate; dmt: 1,2-dithiole-3-thione-4,5-dithiolate.

thermodynamic radius and, as a consequence, they suffer a greater alteration in the ligands arrangement around the central atom.

In Table 6 the Mulliken atomic charges are shown on the metal cations. The results analysis shows that for the monosubstituted complexes the charge on the Zn^{2+} cation is more positive than on the Ni^{2+} cation. As previously shown the metal-ligand binding is predominantly electrostatic in the monosubstituted complexes. Thus, the largest positive charge on the Zn^{2+} cation strengthens the interaction with the dithiolene ligands and justifies the large ionic character. For the disubstituted complexes the positive charge on the metal center is reduced, decreasing the ionic interaction character.

Table 6. Charge on the metals in the aquacomplexes

Ligand	$[M(OH_2)_4(L)] / e $		$[M(OH_2)_2(L)_2]^{2-} / e $	
	Ni^{2+}	Zn^{2+}	Ni^{2+} (Qd)	Zn^{2+} (Td)
Cl ₂ -bdt	1.680	1.853	1.234	1.661
Cl ₄ -bdt	1.735	1.946	1.131	1.509
bdt	1.570	1.632	1.735	1.474
edt	1.083	1.190	1.095	1.050
mdt	1.257	1.414	1.000	1.005
mnt	1.424	1.739	1.655	1.338
tdt	1.783	1.644	1.773	1.328
tfd	1.347	1.644	2.188	1.498
dmit	0.568	0.793	1.800	0.784
dmio	0.541	0.809	1.723	0.956
dmt	0.536	0.804	1.718	0.922

Qd: quadratic; Td: tetrahedral; Cl₂-bdt: 3,6-dichlorobenzene-1,2-dithiolate; Cl₄-bdt: 3,4,5,6-tetrachlorobenzene-1,2-dithiolate; bdt: benzene-1,2-dithiolate; edt: 1,2-ethylenedithiolate; mdt: 1,2-dimethyl-1,2-ethylenedithiolate; mnt: maleonitrile-2,3-dithiolate; tdt: toluene-3,4-dithiolate; tfd: bis(trifluoromethyl)ethylenedithiolate; dmit: 1,3-dithiole-2-thione-4,5-dithiolate; dmio: 1,3-dithiole-2-one-4,5-dithiolate; dmt: 1,2-dithiole-3-thione-4,5-dithiolate.

In Table 7, the softness of the mono- and disubstituted complexes, the aquacations and the ligands studied are listed. According to the Hard and Soft acid-base theory of Pearson,⁴¹ the dithiolene ligands are softer than the $[Ni(OH_2)_6]^{2+}$ (2.11 eV⁻¹) and $[Zn(OH_2)_6]^{2+}$ (1.48 eV⁻¹) cations. The softness (*S*) was calculated, through the difference of orbitals HOMO (*E_H*) and LUMO (*E_L*) energy for each ligand and complex formed using equation 4.

$$S = 1/((E_L - E_H)/2) \quad (4)$$

Natural bond orbital analysis (NBO)

In Table 8, it is listed the energy calculated by the second-order perturbation theory,⁴² which represent the

Table 7. Softness (*S*) of the isolated ligands and the Ni^{2+} and Zn^{2+} aquacomplexes

Ligand	L^{2-} / eV^{-1}	$[M(OH_2)_4(L)] / eV^{-1}$		$[M(OH_2)_2(L)_2]^{2-} / eV^{-1}$	
		Ni^{2+}	Zn^{2+}	Ni^{2+} (Qd)	Zn^{2+} (Td)
Cl ₂ -bdt	17.24	13.33	13.51	4.84	5.28
Cl ₄ -bdt	20.41	12.66	13.16	3.77	5.65
bdt	20.00	14.28	15.62	7.61	6.13
edt	13.89	15.62	16.95	4.88	4.27
mdt	26.31	18.52	20.83	6.24	5.06
mnt	11.11	11.23	9.90	5.98	5.20
tdt	19.23	14.70	17.73	8.41	6.67
tfd	13.16	12.34	13.16	7.81	7.53
dmit	15.38	17.24	21.74	8.26	11.98
dmio	12.36	15.87	21.74	6.72	9.80
dmt	12.34	16.67	21.74	7.72	11.31

Qd: quadratic; Td: tetrahedral; Cl₂-bdt: 3,6-dichlorobenzene-1,2-dithiolate; Cl₄-bdt: 3,4,5,6-tetrachlorobenzene-1,2-dithiolate; bdt: benzene-1,2-dithiolate; edt: 1,2-ethylenedithiolate; mdt: 1,2-dimethyl-1,2-ethylenedithiolate; mnt: maleonitrile-2,3-dithiolate; tdt: toluene-3,4-dithiolate; tfd: bis(trifluoromethyl)ethylenedithiolate; dmit: 1,3-dithiole-2-thione-4,5-dithiolate; dmio: 1,3-dithiole-2-one-4,5-dithiolate; dmt: 1,2-dithiole-3-thione-4,5-dithiolate.

magnitude of the donor-acceptor interactions among the binding orbitals (from the sulfur atoms, a Lewis base) and the anti-binding orbitals (from the metal ion, a Lewis acid). In the first substitution of the Ni^{2+} aquacation, the donor-acceptor energies are asymmetric for each anchor point. This is due to the dipole-dipole interactions among the H atoms of the water ligands and the sulfur atoms of the dithiolates, which leads to weaker interaction. For the Zn^{2+} complexes, the donor-acceptor energies are more symmetric, this may be due to a better octahedral geometric accommodation of the electron density. However, the Ni-ligand donor-acceptor energy values are smaller than those observed for the respective Zn aquacomplexes, resulting in a lower covalent character on the Ni-S bonds. The evaluation of the hybrid orbitals of the sulfur atoms reveal a large p character in the orbital that contributes to the M-L bond. Specifically, for the Zn aquacomplexes the hybrid orbitals also indicate small s orbital hybridization, when compared to nickel.

The evaluation of the second substitution further confirms the covalent character of the Zn-S bonds, but with smaller donor-acceptor energy values compared to the monosubstituted complexes. The donor-acceptor energy is shown in Table 8 for the nickel complexes, a larger donor-acceptor energy values are observed for the second ligand substitution, confirming the largest covalent character and the smallest metal-ligand distance. The analysis of the

Table 8. Donor-acceptor energy ($E_{\text{Donor-Accept}}$) and s, p and d character of the metal-ligand bonding orbital

Ligand (L)		[Ni(OH ₂) ₄ (L)]				[Zn(OH ₂) ₄ (L)]			
		$E_{\text{Donor-Accept}} /$ (kcal mol ⁻¹)	s / %	p / %	d / %	$E_{\text{Donor-Accept}} /$ (kcal mol ⁻¹)	s / %	p / %	d / %
Cl ₂ -bdt	S ₁	29.59	11.26	88.66		98.90	6.46	93.35	
	S ₁		13.20	86.70			2.76	97.04	
	M	35.07	17.40	82.00	0.60	75.88	18.93	80.50	0.57
Cl ₄ -bdt	S ₁	19.23	8.21	91.71		108.76	9.61	90.22	
	S ₁		9.74	90.19			6.11	93.70	
	M	21.42	6.58	93.35	0.07	96.15	18.69	80.75	0.56
bdt	S ₁	35.17	15.29	84.62		120.79	7.75	92.04	
	S ₁		15.87	84.05			7.72	92.13	
	M	33.99	17.71	81.72	0.57	83.97	19.32	80.09	0.59
edt	S ₁	32.67	13.42	86.49		116.99	7.19	92.61	
	S ₁		13.98	85.94			7.38	92.46	
	M	33.00	18.06	81.38	0.56	95.87	18.35	81.07	0.58
mdt	S ₁	33.98	16.46	83.46		113.53	10.74	89.10	
	S ₁		16.61	83.31			8.16	91.68	
	M	33.56	16.46	83.46	0.08	92.80	20.75	78.77	0.48
mnt	S ₁	31.76	11.80	88.11		102.97	9.29	90.56	
	S ₁		11.63	88.29			4.26	95.54	
	M	30.79	16.70	82.67	0.63	88.39	14.19	85.31	0.49
tdt	S ₁	39.13	66.48	33.50		119.55	7.83	91.97	
	S ₁		66.52	33.46			8.00	91.84	
	M	45.58	66.76	33.18	0.06	91.63	19.29	80.13	0.58
tfd	S ₁	30.00	0.06	99.89		112.06	9.58	90.24	
	S ₁		73.84	26.16			3.57	96.25	
	M	33.72	72.18	27.74	0.08	83.40	17.98	81.48	0.55
dmit	S ₁	32.59	11.92	88.00		102.63	7.02	92.80	
	S ₁		11.95	87.96			6.96	92.85	
	M	33.11	17.11	82.26	0.60	107.77	18.32	81.07	0.62
dmio	S ₁	32.76	12.32	87.60		95.36	6.87	92.96	
	S ₁		12.35	87.57			6.68	93.14	
	M	33.35	17.01	82.39	0.60	95.93	18.33	81.10	0.57
dmt	S ₁	32.01	11.91	88.02		93.26	4.75	95.05	
	S ₁		11.04	88.85			7.87	91.94	
	M	36.49	16.97	81.38	0.63	124.51	20.51	78.92	0.56
Cl ₂ -bdt			[Ni(OH ₂) ₂ (L) ₂] ²⁻			[Zn(OH ₂) ₂ (L) ₂] ²⁻			
	S ₁	79.95	12.88	86.95		75.77	11.30	88.62	
	S ₁		12.87	86.96			8.75	91.18	
	S ₂	80.01	12.81	87.01		63.02	11.70	88.20	
	M		2.68	97.14	0.17		15.82	83.73	0.45
Cl ₄ -bdt	S ₁	65.57	8.45	82.76		45.23	8.38	91.57	
	S ₁		8.32	82.78			8.34	91.61	
	S ₂	70.05	8.21	84.03		84.09	11.89	88.04	
	S ₂		8.17	84.06			12.23	87.68	
	M		16.82	82.53	0.65		15.85	83.11	0.64
bdt	S ₁	64.46	14.55	85.33		54.60	9.69	90.25	
	S ₁		14.54	85.34			9.70	90.25	
	S ₂	64.50	14.55	85.33		73.84	7.75	92.14	
	S ₂		13.90	85.94			13.75	86.35	
	M		14.93	84.61	0.46		19.62	79.89	0.50
edt	S ₁	70.97	13.80	86.05		51.43	8.07	91.87	
	S ₁		13.80	86.05			8.79	91.12	
	S ₂	70.99	13.80	86.05		71.43	8.92	90.99	
	S ₂		13.80	86.05			9.43	90.50	
	M		7.81	91.94	0.25		18.96	80.51	0.53

Table 8. Donor-acceptor energy ($E_{\text{Donor-Accept}}$) and s, p and d character of the metal-ligand bonding orbital (cont.)

Ligand (L)	[Ni(OH ₂) ₄ (L)]				[Zn(OH ₂) ₄ (L)]			
	$E_{\text{Donor-Accept}} /$ (kcal mol ⁻¹)	s / %	p / %	d / %	$E_{\text{Donor-Accept}} /$ (kcal mol ⁻¹)	s / %	p / %	d / %
mdt	S ₁	75.02	10.04	89.76	80.92	7.23	92.65	
	S _{1'}	74.95	10.03	89.77	81.52	13.49	86.43	
	S ₂	79.19	14.01	85.83	62.31	11.14	88.80	
	S _{2'}	79.20	14.03	85.82	72.19	11.23	88.70	
	M		19.94	79.70	0.36		13.94	85.79
mnt	S ₁	73.87	2.54	97.13	82.06	10.91	89.00	
	S _{1'}	72.88	2.41	97.26	77.86	10.43	89.49	
	S ₂	74.58	11.79	88.06	64.88	6.85	93.07	
	S _{2'}	74.34	11.78	88.07	58.05	5.91	94.02	
	M		14.11	85.52	0.37		8.94	90.78
tdt	S ₁	77.45	9.81	89.98	60.85	4.48	95.42	
	S _{1'}	77.74	9.93	89.87	65.94	7.59	92.34	
	S ₂	80.49	14.06	85.76	82.08	13.44	86.48	
	S _{2'}	80.48	13.95	85.89	74.03	16.92	82.50	
	M		20.42	78.95	0.63		13.56	86.09
tfd	S ₁	78.92	13.14	86.70	76.51	4.52	95.17	
	S _{1'}	80.75	12.84	86.99	50.63	3.57	96.35	
	S ₂	83.37	8.37	91.40	61.55	6.70	93.23	
	S _{2'}	82.75	6.97	92.78	64.43	3.16	96.69	
	M		6.33	93.39	0.28		13.35	86.30
dmit	S ₁	77.92	8.23	91.56	76.86	10.13	89.78	
	S _{1'}	78.02	8.24	91.55	76.82	10.12	89.79	
	S ₂	78.94	11.96	87.88	72.61	7.62	92.28	
	S _{2'}	78.94	11.96	87.87	85.24	8.14	91.14	
	M		19.04	80.31	0.65		18.69	80.71
dmio	S ₁	61.78	11.02	88.91	76.70	6.62	93.27	
	S _{1'}	62.29	11.16	88.76	73.89	8.76	91.16	
	S ₂	70.96	13.31	86.60	77.09	10.22	89.68	
	S _{2'}	70.76	13.23	86.69	75.42	10.01	89.90	
	M		18.44	80.90	0.65		15.29	84.04
dmt	S ₁	74.85	7.52	92.26	48.41	4.73	95.20	
	S _{1'}	84.08	9.16	90.63	103.87	9.51	90.37	
	S ₂	79.86	10.25	89.53	92.74	9.12	90.77	
	S _{2'}	81.31	9.41	90.39	61.72	16.71	83.23	
	M		18.45	81.20	0.34		18.56	80.79

The S1 and S1' parameters refer to the two S atoms of the bidentate ligand in the monosubstitution case. In the disubstitution case the S2 and S2' parameters refer to the S atoms of the second bidentate ligand; the M parameter refers to the metal ion (Ni or Zn). Cl₂-bdt: 3,6-dichlorobenzene-1,2-dithiolate; Cl₄-bdt: 3,4,5,6-tetrachlorobenzene-1,2-dithiolate; bdt: benzene-1,2-dithiolate; edt: 1,2-ethylenedithiolate; mdt: 1,2-dimethyl-1,2-ethylenedithiolate; mnt: maleonitrile-2,3-dithiolate; tdt: toluene-3,4-dithiolate; tfd: bis(trifluoromethyl)ethylenedithiolate; dmit: 1,3-dithiole-2-thione-4,5-dithiolate; dmio: 1,3-dithiole-2-one-4,5-dithiolate; dmt: 1,2-dithiole-3-thione-4,5-dithiolate.

orbital involved in the metal-ligand interaction shows a pronounced p character in the molecular orbitals where the electron density donated to the metal is located. It is very clear that in the metal-ligand bond lengths, the chelating angles, the charge on the metal center and the softness of the aquacomplexes are strictly related to the effects of the metal-ligand coordination, analyzed from the NBO.

The NBO results indicate that the steric and electron withdrawing effects of the atoms adjacent to the anchoring point, modulate the binding strength of the complexes.

Additionally, the geometric parameters are in good agreement with the NBO analysis. The donor-acceptor energy of the mono substituted Zn²⁺ complexes is larger than the respective Ni²⁺ complexes, showing a larger covalent stabilization. The same analysis for the disubstituted complexes reveals a similar covalent character, based on the donor-acceptor energies. For all the complexes, it is possible to observe that the metal-ligand interaction has a predominant p character. It was also observed a small backdonation from the Ni²⁺ and Zn²⁺ metal centers for the

sulfur atoms of the dithiolene ligands (see Supplementary Information (SI) Table S1). This trend was not observed with the Ca²⁺ and Mg²⁺ aquacomplexes with the same dithiolene ligands because they did not occupy the d orbitals to perform these interactions.¹⁹ The computational results presented here are important for the rational design of dithiolate complexes for a wide range of advanced applications in the fields of coordination chemistry and materials science.

Conclusions

The affinity of bidentate dithiolene ligands for the [Ni(OH₂)₆]²⁺ and [Zn(OH₂)₆]²⁺ complexes was measured by substitution energies and rationalized by geometric, energetic and electronic parameters. As ligands, three sets were evaluated: the aromatic, the double bond (ethylene) and the heterocyclic molecules. Generally, the ethylene dithiolate complexes have more negative enthalpy and Gibbs energy value than the respective phenyl dithiolene complexes. The enthalpy interaction order of interaction is: edt < mdt < tfd < mnt for ethylenic, tdt < bdt < Cl₂-bdt < Cl₄-bdt for the phenyl and dmio < dmt < dmit for the heterocyclic dithiolenes. Those orders are mainly determined by the electronic nature of the functional group. For the first substitution all the Ni²⁺ and Zn²⁺ complexes maintained the octahedral geometry. In the second substitution the Ni²⁺ complexes have quadratic geometry, while the Zn²⁺ complexes have tetrahedral geometry, due to their electronic structure. The EDA results show that dithiolate modulates the electrostatic contribution of the interaction for the first substitution and the covalent interaction for the second substitution in both metal ions.

The EDA method shows that the differences in the ligands ability to coordinate with the metal center are reflected mainly in the electrostatic component of the interaction energy, which is the main term for the first substitution of the ligand for Ni²⁺ and Zn²⁺. The exchange and dispersion components are almost constant for the series of the analyzed ligands, while the Pauli repulsion varies by about a quarter of the range of the electrostatic interaction term. The metal-ligand bonding lengths, the chelation angles, the charge at the metal center and the softness of the aquacomplexes are strictly correlated with the metal-ligand coordination force.

The NBO results indicate that the steric and electron retraction effects of the atoms adjacent to the metal-ligand coordination modulate the binding strength of the complexes, as well as the geometric parameters are in good agreement with the NBO analysis. The donor-receptor energy of the monosubstituted Zn²⁺ complexes is

larger than that of the respective Ni²⁺ complexes, showing a larger covalent stabilization. In the second substitution, this trend is maintained, but with a smaller magnitude. For all the analyzed complexes, the p character of the metal-ligand interactive orbital is the predominant one. The computational results presented here are important to rationalize the nature of the metal ligand interaction in dithiolene complexes and then contribute to development of model compounds for various advanced applications.

Supplementary Information

Supplementary data (donor-acceptor energy for metal-ligand backdonation selected) are available free of charge at <http://jbcs.sbcq.org.br> as PDF file.

Acknowledgments

Dr Glaucio B. Ferreira and Dr Leonardo M. da Costa acknowledge FAPERJ (Fundação de Amparo à Pesquisa do Estado do Rio de Janeiro) and CNPq (Conselho Nacional de Desenvolvimento Científico e Tecnológico).

References

1. Belo, D.; Almeida, M.; *Coord. Chem. Rev.* **2010**, *254*, 1479.
2. Hine, F. J.; Taylor, A. J.; David Garner, C.; *Coord. Chem. Rev.* **2010**, *254*, 1570.
3. Pilarczyk, K.; Daly, B.; Podborska, A.; Kwolek, P.; Silverson, V. A. D.; de Silva, A. P.; Szacitowski, K.; *Coord. Chem. Rev.* **2016**, *325*, 135.
4. Holm, R. H.; *Inorg. Chem.* **2007**, *46*, 4090.
5. Mtei, R. P.; Perera, E.; Mogesa, B.; Stein, B.; Basu, P.; Kirk, M. L.; *Eur. J. Inorg. Chem.* **2011**, *36*, 5467.
6. Musiani, F.; Gioia, D.; Masetti, M.; Falchi, F.; Cavalli, A.; Recanatini, M.; Ciurli, S.; *J. Chem. Theory Comput.* **2017**, *13*, 2322.
7. Lindahl, M.; Tagesson, C.; *Inflammation* **1996**, *20*, 599.
8. Famengo, A.; Pinero, D.; Jeannin, O.; Guizouarn, T.; Piekara-Sadye, L.; Fourmigué, M.; *New J. Chem.* **2012**, *36*, 638.
9. Zhang, Z.; Yang, T.; Qin, P.; Dang, L.; *J. Organomet. Chem.* **2018**, *864*, 143.
10. Singh, M. K.; Sutradhar, S.; Paul, B.; Adhikari, S.; Laskar, F.; Acharya, S.; Chakraborty, D.; Biswas, S.; Das, A.; Roy, S.; Frontera, A.; *J. Mol. Struct.* **2018**, *1164*, 334.
11. Bhat, M. A.; Lone, S. H.; Butcher, R. J.; Srivastava, S. K.; *J. Mol. Struct.* **2018**, *1168*, 242.
12. Soras, G.; Psaroudakis, N.; Manos, M. J.; Tasiopoulos, A. J.; Liakos, D. G.; Mousdis, G. A.; *Polyhedron* **2013**, *62*, 208.
13. Soras, G.; Psaroudakis, N.; Manos, M. J.; Tasiopoulos, A. J.; Liakos, D. G.; Mousdis, G. A.; *Polyhedron* **2009**, *28*, 3340.

14. Drzewiecka-Antonik, A.; Ferenc, W.; Wolska, A.; Klepka, M. T.; Cristóvão, B.; Sarzyński, J.; Rejmak, P.; Osypiuk, D.; *Chem. Phys. Lett.* **2017**, *667*, 192.
15. Xia, Y.; Miao, Z.; Wang, F.; Yao, H.; Cui, M.; Ma, Y.; Qi, Z.; Sun, Y.; *J. Organomet. Chem.* **2015**, *779*, 81.
16. Plazinski, W.; Drach, M.; *J. Phys. Chem. B* **2013**, *117*, 12105.
17. Tavasoli, E.; Fattahi, A.; *J. Theor. Comput. Chem.* **2009**, *8*, 475.
18. Quattrociochi, D. G. S.; Ferreira, G. B.; da Costa, L. M.; Carneiro, J. W. M.; *Comput. Theor. Chem.* **2016**, *1075*, 104.
19. Melengate, G. S.; Stoyanov, S. R.; Quattrociochi, D. G. S.; da Costa, L. M.; Ferreira, G. B.; *J. Braz. Chem. Soc.* **2017**, *29*, 856.
20. Dudev, M.; Wang, J.; Dudev, T.; Lim, C.; *J. Phys. Chem. B* **2006**, *110*, 1889.
21. Persson, I.; *Pure Appl. Chem.* **2010**, *82*, 1901.
22. Corral, I.; Mo, O.; Yanez, M.; Scott, A.; Radom, L.; *J. Phys. Chem. A* **2003**, *107*, 10456.
23. Corral, I.; M6, O.; Yáñez, M.; Salpin, J.; Tortojada, J.; Moran, D.; Radom, L.; *Chem.-Eur. J.* **2006**, *12*, 6787.
24. Corral, I.; M6, O.; Yáñez, M.; Salpin, J.; Tortojada, J.; Radom, L.; *J. Phys. Chem. A* **2004**, *108*, 10080.
25. Trujillo, C.; Lamshabi, A. M.; M6, O.; Yáñez, M.; *Phys. Chem. Chem. Phys.* **2008**, *10*, 3229.
26. Andrew, F. P.; Ajibade, P. A.; *J. Mol. Struct.* **2018**, *1155*, 843.
27. Nanjundam, N.; Narayanasamy, R.; Butcher, R. J.; Jasinski, J.; Velmurugan, K.; *Inorg. Chim. Acta* **2017**, *455*, 283.
28. Lee, C.; Yang, W.; Parr, R. G.; *Phys. Rev. B* **1988**, *37*, 785.
29. Hehre, W. J.; Radom, L.; Schleyer, P. V. R.; Pople, J. A.; *Ab Initio Molecular Orbital Theory*, vol. 7; Wiley: New York, USA, 1989.
30. Frisch, M. J.; Trucks, G. W.; Schlegel, H. B.; Scuseria, G. E.; Robb, M. A.; Cheeseman, J. R.; Scalmani, G.; Barone, V.; Mennucci, B.; Petersson, G. A.; Nakatsuji, H.; Caricato, M.; Li, X.; Hratchian, H. P.; Izmaylov, A. F.; Bloino, J.; Zheng, G.; Sonnenberg, J. L.; Hada, M.; Ehara, M.; Toyota, K.; Fukuda, R.; Hasegawa, J.; Ishida, M.; Nakajima, T.; Honda, Y.; Kitao, O.; Nakai, H.; Vreven, T.; Montgomery Jr., J. A.; Peralta, J. E.; Ogliaro, F.; Bearpark, M.; Heyd, J. J.; Brothers, E.; Kudin, K. N.; Staroverov, V. N.; Kobayashi, R.; Normand, J.; Raghavachari, K.; Rendell, A.; Burant, J. C.; Iyengar, S. S.; Tomasi, J.; Cossi, M.; Rega, N.; Millam, J. M.; Klene, M.; Knox, J. E.; Cross, J. B.; Bakken, V.; Adamo, C.; Jaramillo, J.; Gomperts, R.; Stratmann, R. E.; Yazyev, O.; Austin, A. J.; Cammi, R.; Pomelli, C.; Ochterski, J. W.; Martin, R. L.; Morokuma, K.; Zakrzewski, V. G.; Voth, G. A.; Salvador, P.; Dannenberg, J. J.; Dapprich, S.; Daniels, A. D.; Farkas, Ö.; Foresman, J. B.; Ortiz, J. V.; Cioslowski, J.; Fox, D. J.; *Gaussian 09, Revision E.01*, Gaussian, Inc., Wallingford CT, 2009.
31. Hu, L.; Chen, K.; Chen, H.; *J. Chem. Theory Comput.* **2017**, *13*, 4841.
32. Boys, S. F.; Bernardi, F.; *Mol. Phys.* **1970**, *19*, 553.
33. Schmidt, M. W.; Baldrige, K. K.; Boatz, J. A.; Elbert, S. T.; Gordon, M. S.; Jensen, J. H.; Koseki, S.; Matsunaga, N.; Nguyen, K. A.; Su, S.; Windus, T. L.; Dupious, M.; Montgomery, J. A.; *J. Comput. Chem.* **1993**, *14*, 1347.
34. Gordon, M. S.; Schmidt, M. W. *In Theory and Applications of Computational Chemistry: The First Forty Years*; Dykstra, C. E.; Frenking, G.; Kim, K. S.; Scuseria, G. E., eds.; Elsevier: Amsterdam, 2005, p. 1167.
35. Su, P.; Li, H.; *J. Chem. Phys.* **2009**, *131*, 014102.
36. Schmidt, M. W.; Baldrige, K. K.; Boatz, J. A.; Elbert, S. T.; Gordon, M. S.; Jensen, J. H.; Koseki, S.; Matsunaga, N.; Nguyen, K. A.; Su, S.; Windus, T. L.; Dupious, M.; Montgomery, J. A.; *J. Comput. Chem.* **1993**, *14*, 1347.
37. Yua, S. S.; Zhanga, H.; *Acta Crystallogr.* **2016**, *72*, 1197.
38. Hancock, R. D.; Martell, A. E.; *Chem. Rev.* **1989**, *89*, 1875.
39. Vallet, V.; Wahlgren, U.; Grenthe, I.; *J. Am. Chem. Soc.* **2003**, *125*, 14941.
40. Greene, C.; Grudzien, P. K.; York, J. T.; *J. Organomet. Chem.* **2017**, *851*, 122.
41. Pearson, R. G.; *J. Am. Chem. Soc.* **1963**, *85*, 3533.
42. Anderson, K.; Malmqvist, P. A.; Roos, B. O.; *J. Chem. Phys.* **1991**, *96*, 1218.

Submitted: December 4, 2018

Published online: January 23, 2019

